Journal of Power Sources, 43–44 (1993) 595–602

The cycling properties of the $Li_xNi_{1-y}Co_yO_2$ electrode

C. Delmas*, I. Saadoune and A. Rougier

Laboratoire de Chimie du Solide du CNRS and Ecole Nationale Supérieure de Physique et Chimie de Bordeaux, Université Bordeaux I, 351 cours de la Libération, 33405 Talence Cedex (France)

Abstract

The $LiNiO_2$–$LiCoO_2$ system exhibits a complete solid solution. These materials crystallize in the rhombohedral system with a layered structure. They have been used as positive electrode in lithium batteries. Up to 0.5 lithium atom can be reversibly deintercalated in the 3.5 to 4.0 V potential range. The highest specific energy (close to 500 W h/kg) is obtained in the $Li_xNi_{0.7}Co_{0.3}O_2$ system. Moreover, the very small volume change upon deintercalation increased their interest for application point of view.

Introduction

Reversible intercalation/deintercalation reactions, especially those involving lithium in the layered transition metal oxides AMO_2, have generated considerable interest in the last few years because of the use of these lamellar oxides as positive electrode materials in high energy density secondary batteries [1–3]. Among these electrode materials, Li_xNiO_2 and Li_xCoO_2 have been intensively studied due to their very promising electrochemical performances [4–8].

Li_xCoO_2 system has been studied more extensively compared with Li_xNiO_2 because of the two important reasons. Firstly, pure $LiCoO_2$ phase is relatively easy to prepare and secondly, the cell obtained making use of Li_xCoO_2 offers a considerably high voltage owing to the oxidizing power of Co^{4+}/Co^{3+} redox couple. If the second reason can be regarded as an advantage for the specific energy, it poses problem from the application point of view as the electrolyte is not very stable at such high voltages.

On the other hand, it has been shown that for $x < 0.5$, some structural irreversible rearrangements of the Li_xNiO_2 phases occur leading to a modification of the electrochemical behaviour of the Li/Li_xNiO_2 cell [4].

The use of the solid solution between $LiCoO_2$ and $LiNiO_2$ appears to be much more promising. In this paper, we report on the structural and electrochemical investigations of the $Li_xNi_{1-y}Co_yO_2$ solid solution with nickel-rich phases.

Experimental

A series of compounds in the $LiNi_{1-y}Co_yO_2$ system ($0 \leqslant y \leqslant 1$) were prepared by heating a pelletized stoichiometric mixture of Li_2CO_3, NiO and Co_3O_4, under dry

*Author to whom correspondence should be addressed.

0378-7753/93/$6.00

oxygen, in the 600 to 900 °C temperature range depending on the y value, with intermittent grindings. It should be noted that the stoichiometry and the cationic distribution are highly sensitive to the experimental conditions.

The electrochemical measurements were carried out in cells exhibiting the following electrochemical chain: Li/$LiClO_4$ (1 M) in propylene carbonate (PC)/$Li_xNi_{1-y}Co_yO_2$. These cells, assembled in a dry box, have been galvanostatically cycled in the 70 to 500 $\mu A/cm^2$ current density range. In order to avoid an electrolyte degradation, the upper potential threshold was limited at 4.0 V. After electrochemical cycling, the cathodic materials were taken out from the cells and characterized by X-ray powder diffractometry.

Results and discussion

Structural characterization of the $LiNi_{1-y}Co_yO_2$ starting phases

In the whole composition range ($0 \leqslant y \leqslant 1$), a pure phase $LiNi_{1-y}Co_yO_2$ has been obtained. The X-ray diffractograms of all the samples are characteristic of the α-$NaFeO_2$ type structure (SG: $R\bar{3}m$) (O3 type structure [9]). Transition metal ions

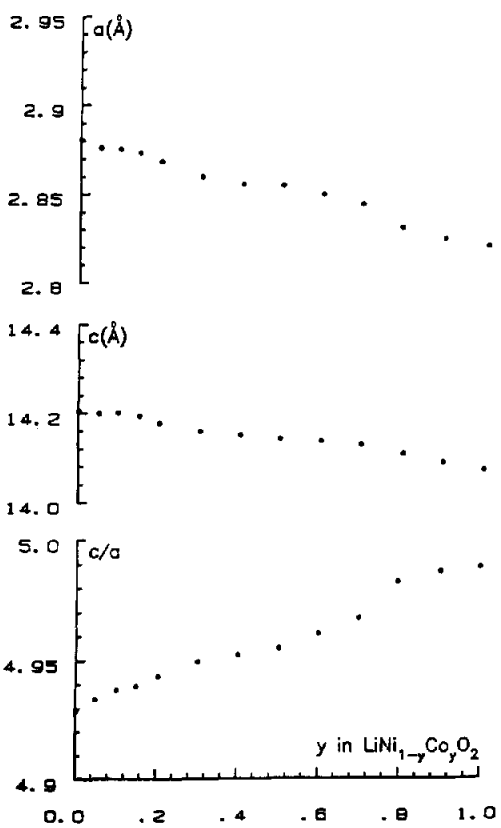

Fig. 1. Variation of the hexagonal cell parameters and of c/a ratio vs. y in the $LiNi_{1-y}Co_yO_2$ solid solution.

are surrounded by six oxygen atoms forming $Ni_{1-y}Co_yO_2$ infinite slabs by edge-sharing of the ($Ni_{1-y}Co_yO_6$) octahedra. Lithium ions are located between the $Ni_{1-y}Co_yO_2$ layers in octahedral sites. Lattice parameters of the hexagonal cell, which were obtained from a least squares refinement, and c/a ratio are reported in Fig. 1.

The a parameter, related to the intralayer metal–metal distance, decreases continually with y as a result of the difference in size between the trivalent cobalt and nickel ions ($r_{Ni^{III}} = 0.56$ Å, $r_{Co^{III}} = 0.53$ Å) [10]. It should be noticed that the variation is not completely monotonous. This evolution can be related to that of the magnetic properties versus y [11].

In the same way, the c parameter, equal to three times the interslab distance, decreases slowly when y increases.

The c/a ratio which characterizes the structure anisotropy increases when trivalent cobalt is substituted for nickel ($c/a = 2\sqrt{6}$ for a cubic lattice). This variation suggests that the substitution of cobalt for nickel increases the 2D character of the structure. It has already been noted that stoichiometric $LiNiO_2$ is difficult to prepare. The true formula of this nickelate is $Li_{1-z}Ni_{1+z}O_2$ which requires the presence of z nickel atoms in the lithium layer [12, 13]. The cationic distribution in $LiNi_{1-y}Co_yO_2$ ($0 \leqslant y \leqslant 0.3$) oxides was studied by Rietveld refinement of the X-ray data. The detailed results will be reported in a forthcoming paper [14]. For $y = 0$, 4% of nickel ions are located in the lithium layer. The amount of extra nickel ions, which is present between the $Ni_{1-y}Co_yO_2$ slabs, decreases as y increases. Thus, the structure of $LiNi_{0.7}Co_{0.3}O_2$ phase is completely ordered with pure lithium in the interslab space.

Electrochemical behaviour

The $LiNi_{1-y}Co_yO_2$ phases have been used as a positive electrode in lithium batteries and tested electrochemically. Figure 2 shows the thermodynamic curve of the Li/$Li_xNi_{0.8}Co_{0.2}O_2$ cell, obtained by intermittent charge (or discharge) and relaxation steps (the relaxation period was interrupted when the slope of the voltage–time curve was smaller than 0.1 mV/h). In the main part of the intercalation range, the cell polarization is very small as illustrated by the cell voltage–time curve given in Fig. 2(a). This behaviour suggests that these materials would exhibit a high mixed conductivity. The increase in polarization observed at the end of discharge (Fig. 2(b)) results of the well-known reintercalation difficulty due to the low ionic conductivity when the main part of the available sites are occupied.

The similarity in the electrochemical behaviour between the charge and discharge curves shows a very good reversibility of the intercalation/deintercalation process in these materials. Such reversibility is confirmed by a perfect superposition of the second charge with the first charge (Fig. 3). This result shows that the liquid electrolyte ($LiClO_4$ in PC) is completely stable up to 4 V in this cell configuration.

On the other hand, the monotonous variation of the potential–composition curve characterizes the existence of a $Li_xNi_{0.8}Co_{0.2}O_2$ solid solution.

X-ray characterization of the deintercalated phases

The sequence of the powder X-ray diffraction patterns for some $Li_xNi_{0.8}Co_{0.2}O_2$ phases ($x = 1.0$, 0.8, 0.6 and $x = 0.5$), obtained electrochemically, are summarized in Fig. 4. The splitting between the (018) and (110) diffraction lines shows clearly the cell-parameter variation upon intercalation. All materials gave sharp X-ray powder patterns indicating the maintenance of a good crystallinity during the electrochemical

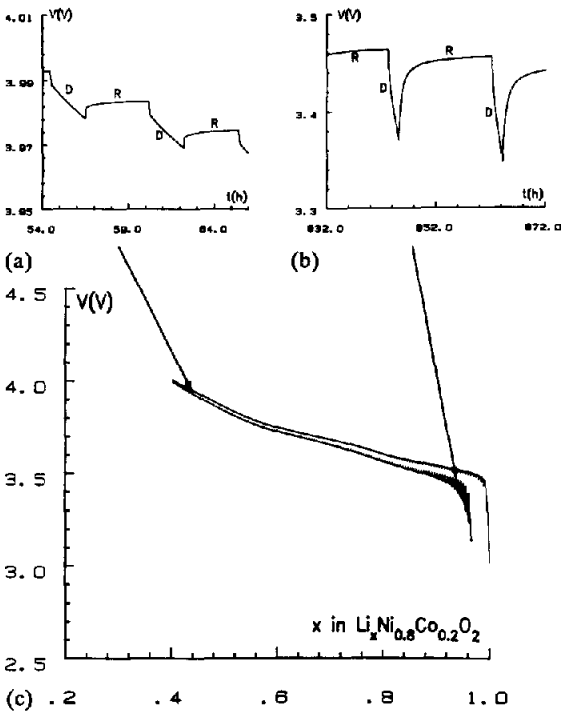

Fig. 2. Variation of the cell potential during a charge with relaxation of a $Li/Li_xNi_{0.8}Co_{0.2}O_2$ cell. The variations of the cell voltage vs. time are given in insets (a) and (b). They show that for a same discharge (D) time a longer relaxation time (R) is required at the end of the intercalation process.

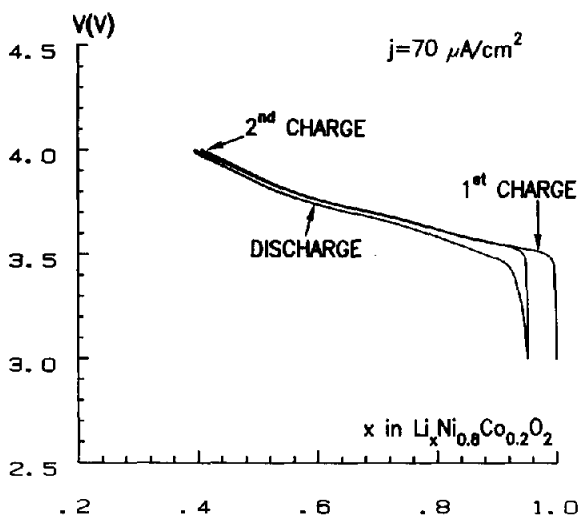

Fig. 3. Comparison between the first and second charge curves of a $Li/Li_xNi_{0.8}Co_{0.2}O_2$ cell.

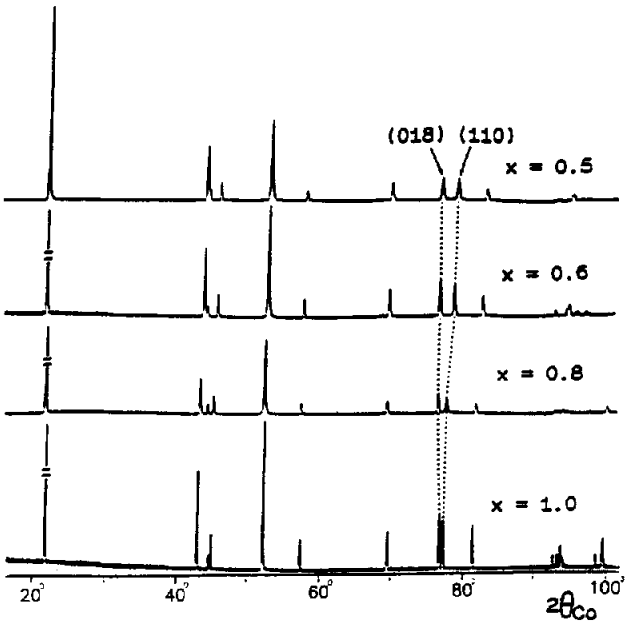

Fig. 4. X-ray powder diffraction patterns of the $Li_xNi_{0.8}Co_{0.2}O_2$ phases ($x = 1.0$, 0.8, 0.6 and 0.5).

TABLE 1

Hexagonal cell parameters and volumes of various $Li_xNi_{1-y}Co_yO_2$ phases

Composition	a (Å)	c (Å)	Volume (Å)^3	Reference
$LiNiO_2$	2.881	14.19	101.9	8
$Li_{0.8}NiO_2$	2.875	14.25	102.0	8
$Li_{0.5}NiO_2$	2.822	14.32	98.8	4
$LiNi_{0.8}Co_{0.2}O_2$	2.875	14.20	101.6	14
$Li_{0.8}Ni_{0.8}Co_{0.2}O_2$	2.855	14.27	100.7	14
$Li_{0.5}Ni_{0.8}Co_{0.2}O_2$	2.825	14.34	99.1	14
$LiNi_{0.1}Co_{0.9}O_2$	2.818	14.06	96.7	14
$Li_{0.8}Ni_{0.1}Co_{0.9}O_2$	2.810	14.17	96.9	14
$Li_{0.5}Ni_{0.1}Co_{0.9}O_2$	2.801	14.34	97.4	14
$LiCoO_2$	2.816	14.08	96.7	6
$Li_{0.74}CoO_2$	2.812	14.22	97.4	6
$Li_{0.5}CoO_2$	2.807	14.42	98.4	6

deintercalation. Furthermore, the similarity between the X-ray patterns shows that the layered structure is preserved on removal of the lithium atoms. This data confirms the topotactic character of the intercalation/deintercalation reaction in this family of oxides.

The hexagonal cell parameters of several $Li_xNi_{1-y}Co_yO_2$ deintercalated phases ($y = 0.0$, 0.2, 0.9, 1.0) are listed in Table 1. In all cases, the a parameter (intralayer metal–metal distance) decreases whereas the c parameter (interslab distance) increases

with decreasing lithium amount. This evolution is in good agreement with the data reported in most A_xMO_2 layered oxides [15, 16] and can be explained respectively by the increase of covalency in the $(Ni_{1-y}Co_yO_2)$ sheets and the loss of the lattice cohesion as x decreases.

The volume of the hexagonal cells have also been reported in Table 1. In both cases, the variation of the volume with the lithium amount is very small. However, it can be noted that the volume decreases with the amount of lithium in the cases of Li_xNiO_2 and $Li_xNi_{0.8}Co_{0.2}O_2$, whereas it increases in the cases of $Li_xNi_{0.1}Co_{0.9}O_2$ and Li_xCoO_2. This remark suggests that there is an intermediate y value ($0.2 \leqslant y \leqslant 0.9$) for which the cell volume remains constant during the intercalation/deintercalation reaction. This point is extremely important for the application of this system in real batteries. For comparison, the unit-cell volume of $LiTiS_2$ is 11% larger than that of the pristine chalcogenide [17].

A general study of the electrochemical behaviour of all $Li_xNi_{1-y}Co_yO_2$ phases shows that the $Li/Li_xNi_{0.7}Co_{0.3}O_2$ cell presents the best cycling properties; the completely-ordered structure (ideal α-$NaFeO_2$ type structure) of the starting material offers good conditions for the lithium diffusion in the interslab space. Thereby, the $Li/Li_xNi_{0.7}Co_{0.3}O_2$ cell has been cycled under different current densities. As shown in Fig. 5, when the current density increases from 70 ($C/200$) to 400 $\mu A/cm^2$ ($C/35$), the capacity decreases slowly with increasing polarization, and, then, decreases notably above 550 $\mu A/cm^2$ ($C/25$). This decrease in capacity, when the cycling rate increases, results mainly from the upper limit of voltage which has been maintained equal to 4.0 V in all experiments. When the charge rate increases, the cell polarization increases, the upper limit voltage

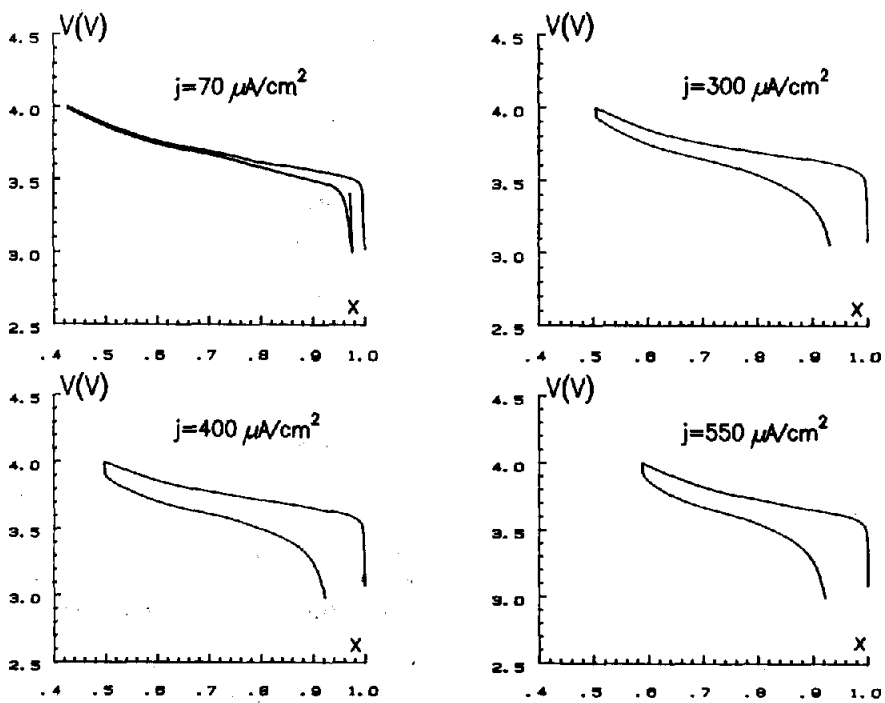

Fig. 5. Potential–composition curves of a $Li/Li_xNi_{0.7}Co_{0.3}O_2$ cell for various current densities.

is more rapidly reached and in those conditions, the cell capacity decreases rapidly. Nevertheless, the high current rate has not affected the reversibility of the cell.

One of the cells has been cycled, with a current of 400 μA/cm^2 for several charge/discharge cycles. The typical voltage–composition curve and the variation, with the cycle number, of the energy density (W h/kg of active electrode material) are illustrated in Fig. 7. The capacity of the first charge is about 15% higher than that of the subsequent cycles and remains constant for the following cycles. As a result, the cell polarization is quite small and the reversibility is preserved with no significant loss in the energy density during the cycling. The experimental energy density recovered on discharge are close to 500 W h/kg. This value is very promising for applications.

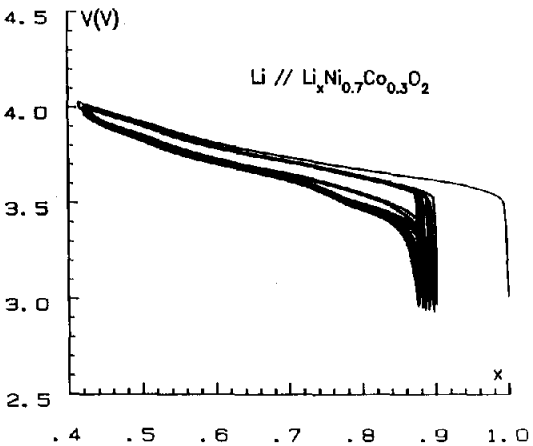

Fig. 6. Cycling behaviour of Li/Li$_x$Ni$_{0.7}$Co$_{0.3}$O$_2$ cell under 400 μA/cm^2.

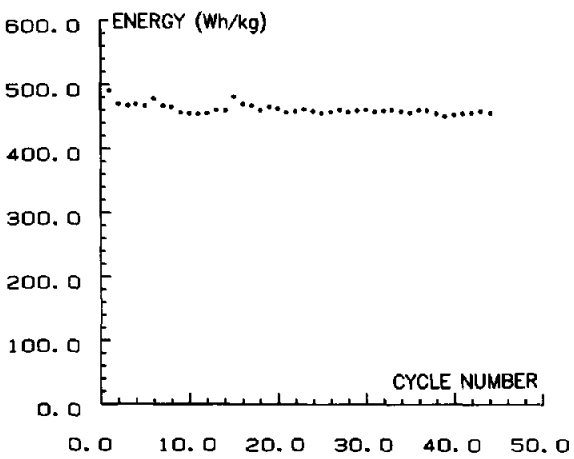

Fig. 7. Variation of the energy density (relative to the electrode material) of a Li/Li$_x$Ni$_{0.7}$Co$_{0.3}$O$_2$ cell vs. cycle number.

Acknowledgement

The authors thank CNES for its financial support.

References

1 S. Miyazaki, S. Kikkawa and M. Koizumi, *Synth. Met., 6* (1983) 211.
2 S. H. Chang, H. H. Park, A. Maazaz and C. Delmas, *C.R. Acad. Sci. Paris, Ser. II, 308* (1989) 475.
3 J. J. Braconnier, C. Delmas and P. Hagenmuller, *Mater. Res. Bull., 17* (1982) 993.
4 M. G. S. R. Thomas, W. I. F. David, J. B. Goodenough and P. Groves, *Mater. Res. Bull., 20* (1985) 1137.
5 J. B. Goodenough, K. Mizushima and T. Takeda, *Jpn J. Appl. Phys., 19-3* (1980) 305.
6 K. Mizushima, P. C. Jones, P. J. Wiseman and J. B. Goodenough, *Mater. Res. Bull., 15* (1980) 783.
7 E. Plichta, M. Salomon, S. Slane, M. Uchiyama, D. Chua, W. B. Ebner and H. W. Lin, *J. Power Sources, 21* (1987) 25.
8 J. R. Dahn, U. Von Sacken and C. A. Michael, *Solid State Ionics, 44* (1990) 87.
9 C. Delmas, J. J. Braconnier, C. Fouassier and P. Hagenmuller, *Solid State Ionics, 3/4* (1981) 165.
10 R. D. Shannon and G. T. Prewitt, *Acta Crystallogr., Sect. B, 25* (1969) 925.
11 I. Saadoune, *Thesis,* University of Bordeaux I, France, 1992.
12 L. D. Dyer, B. S. Borie, J. R. and J. P. Smith, *J. Am. Chem. Soc., 76* (1954) 1499.
13 J. B. Goodenough, D. G. Wickham and W. J. Croft, *J. Phys. Chem. Solids, 5* (1958) 107.
14 I. Saadoune, A. Rougier and C. Delmas, in press.
15 J. J. Braconnier, *Thesis,* University of Bordeaux I, France, 1983.
16 G. Dutta, A. Manthiram, J. C. Grenier and J. B. Goodenough, *J. Solid State Chem.,* submitted for publication.
17 M. S. Whittingham, *Science, 192* (1976) 1126.